BASIC PHYSICAL AND CHEMICAL PROCESSES IN SPACE RADIATION EFFECTS ON POLYMERS

E. Kamaratos
Department of Chemistry
Christopher Newport College
Newport News, VA 23606

J. W. Wilson
NASA Langley Research Center
Hampton, VA 23665

C. K. Chang
Department of Chemistry
Christopher Newport College
Newport News, VA 23606

Y. J. Xu
Department of Physics
Old Dominion University
Norfolk, VA 23508

Large Space Systems Technology - 1981
Third Annual Technical Review
November 16-19, 1981

SPACE RADIATION PHYSICS AND CHEMISTRY

Space ionizing radiation-induced changes in a structural material are initiated by energetic charged particle impact which transfers kinetic energy of the particle via its coulomb field into electronic excitation energy of the material. In complex molecules, the electronic energy is usually shared among various vibrational modes through potential surface crossing phenomena which depend intimately on the molecular structure (ref. 1). Radicals produced through bond rupture are usually placed on a highly repulsive potential surface which may subsequently lead to reactions not accessible at thermal energies in the early phases. The time progression proceeds under conditions of near thermal equilibrium after <1 nsec and reactions are akin to the more usual chemical processes (ref. 2). In the solid state, long lived radicals result from their lack of mobility and chemical activity ends only after long time periods which depend on the temperature. It is natural for laboratory studies to begin with final chemical products to infer events leading to their production. It is more natural from a physicist's point of view to consider the initial impact and energy handling processes. In the future we should meet in the middle of the diagram with some understanding of the radiation degradation of polymers. In the present report we are interested mainly in the energy absorption and the immediately following events.

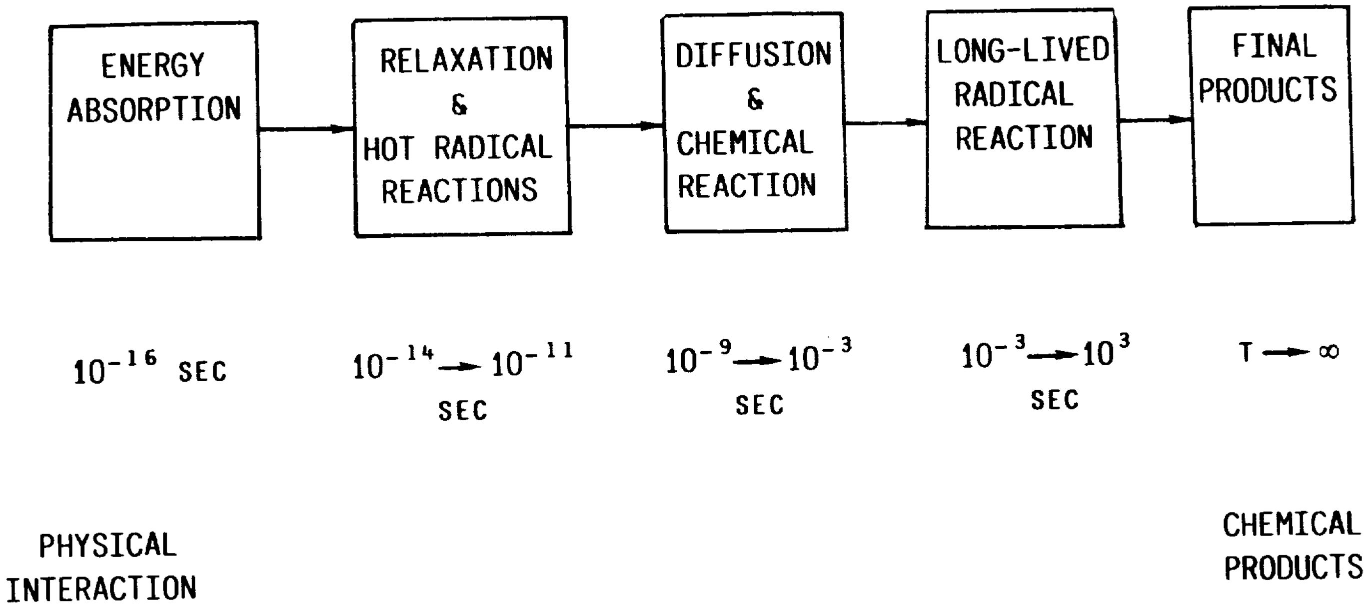

ENERGY ABSORPTION

There are three major questions concerning the energy absorption event. First we should consider how the energy is imparted to the molecule followed by the second question of how the energy was handled by the system leading to the final collision products. These final collision products are the chemically active species which lead to the ultimate change in the material. Of nearly equal importance to what is produced is the third question relating to the spatial distribution of various product types in relation to the charged particle trajectory. We shall consider these questions in more detail.

ENERGY ABSORPTION

A) INTO WHAT MOLECULAR MODES OF THE POLYMER IS THE ENERGY DEPOSITED?

B) WHAT ARE THE CORRESPONDING COLLISION PRODUCTS?

C) WHAT IS THE SPATIAL DISTRIBUTION OF THESE COLLISION PRODUCTS?

COLLISIONAL ENERGY LOSS IN POLYMERS

The energy transferred per unit distance traveled by a passing charged particle to molecules as derived by Bethe (ref. 3) is shown. That the passing coulomb field appears as a field of virtual photons is evidenced by the strong dependence of the stopping power on the optical dipole oscillator strengths, f_n, and the corresponding excitation enery levels, E_n. As chemical bonds are altered, there is a shift in the excitation energies, E_n, and a shift in oscillator strengths as well (ref. 4), consequently the energy deposit depends on the specific molecular structure. The energy deposit, dE, over a distance, dx, of the trajectory is spread laterally from the particle path according to cylindrical symmetry. Ehrenfest's theorem requires the interaction time to be short compared to the oscillator's period and empirically the photon transfer probability to a level E_n is given (ref. 5) by P_n. Clearly the most energetic molecular states are excited near the particle path and the lateral extent of excitation expands with increasing particle velocity. Note that the high energy ionization processes (i.e. large E_n) lie nearest the particle path but the energetic secondary electrons migrate far from the initial particle trajectory (ref. 6). A fundamental quantity is the mean excitation energy, I, which is related to dipole oscillator strengths, f_n, and energy levels, E_n, as shown. This quantity will be studied for effects due to chemical bonding.

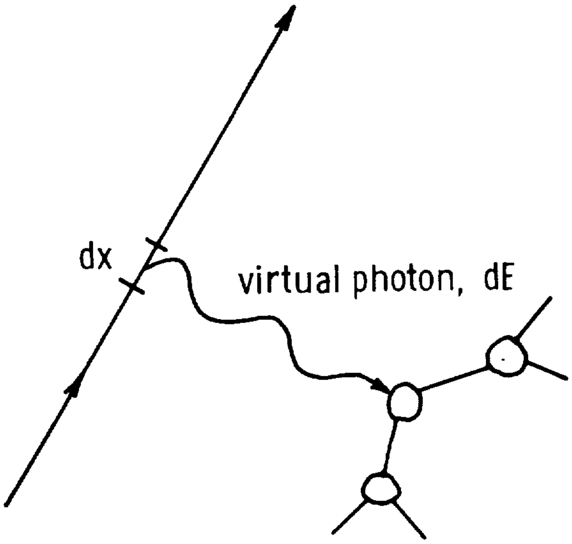

STOPPING POWER

$$\frac{DE}{DX} = [\frac{4\pi N Z_1^2 E^4}{MV^2}] \sum_N F_N \ell N [\frac{2MV^2}{E_N}]$$

LATERAL EXTENT

$$P_N = EXP [-(\frac{E_N}{3HV}) R]$$

FUNDAMENTAL QUANTITY

$$Z \ell N(I) = \sum_N F_N \ell N(E_N)$$

LOCAL PLASMA MODEL FOR POLYMERS

The calculation of excitation energies and oscillator strengths of polymers is beyond present day computational ability. Considerable simplification can be made through replacement of the molecule by an equivalent spatial dependent plasma (ref. 7). The stopping power is now expressed in terms of the local plasma density, $\rho(r)$, and the corresponding plasma frequency, ω_p. The lateral extent of the energy deposit, P_p, and the mean excitation energy, I, are now also given in terms of the local plasma model. To effectively use this model for molecular calculations, means of simple approximation to the electron density of the molecule must be found. For this purpose we used the Gordon-Kim electron gas model (ref. 8) of molecular bonds for the estimation of chemical bond effects (refs. 9-10). The main value of the local plasma model is it's utter simplicity. The accuracy of the local plasma model is tested here by applying the relation between the mean excitation energy, I, and the local plasma density as a fundamental quantity to ionizing radiation interaction.

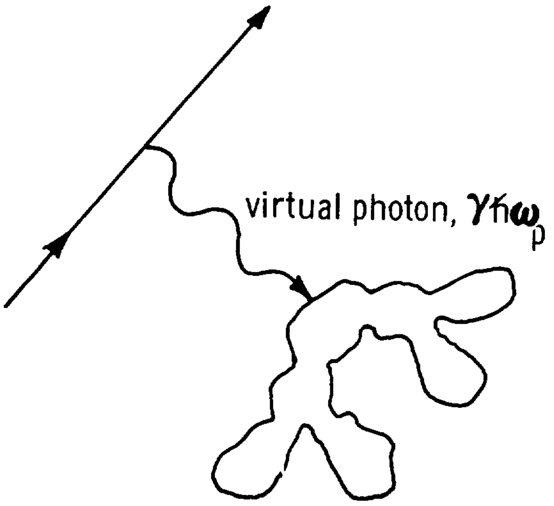

STOPPING POWER

$$\frac{DE}{DX} = \left[\frac{4\pi N Z_1^2 E^4}{MV^2}\right] \int \rho(R)\ \ell N \left[\frac{2MV}{\gamma H\omega_P}\right] D^3R$$

$$\omega_P = \sqrt{4\pi E^2 \rho(R)/M}$$

LATERAL EXTENT

$$P_P \sim \mathrm{EXP}\left[-\left(\frac{\gamma H\omega_P}{3HV}\right) R\right]$$

FUNDAMENTAL QUANTITY

$$Z\ \ell N(I) = \int \rho(R)\ \ell N\ (\gamma H\omega P)\ D^3R$$

CHEMICAL BOND EFFECTS ON MEAN EXCITATION ENERGIES

The mean excitation energies of several molecules related to the polymer problem have been calculated according to the local plasma approximation. The values labeled "atomic" are those obtained using the Bragg rule (ref. 11), in which chemical bond effects are neglected, with the accurate atomic values of Inokuti and coworkers (ref. 12). The present theoretical results are shown for comparison. In addition, experimental results are also shown for which the merit of the present theory is clearly displayed. We conclude from these comparisons that the local plasma model gives an adequate representation of particle impact with the polymer, although the coupling between the electronic mode excited and the remaining vibrational-rotational modes of the polymer are yet undetermined. In search of empirical evidence of the polymer's reaction to the impact we have examined specific fragmentation data from mass spectroscopy.

$$I = \mathrm{EXP}\,[Z^{-1} \int \rho(R)\ \ell N\left(\gamma H \omega_P\right) D^3R]$$

	ATOMIC	PRESENT THEORY	EXPERIMENTAL
CH_4	35.1	44.7	42.8
$(CH_2)_x$	43.5	55.0	53.4
C_6H_6	50.6	60.6	61.4±1.9
H_2	15.0	18.9	18.5±0.5
GRAPHITE	62.0	76.1	78.5±1.5

STRUCTURE OF AN EPOXY POLYMER

A repeating unit is shown in the structure of an epoxy resin produced by curing tetraglycidyl methylenedianiline with diamino diphenyl sulfone (ref. 13). This resin is one of the resins that are reported to be under investigation for possible use in composite materials for applications ranging from Army materiel to aircraft and space structures. An interesting characteristic of this polymer is the presence of several tertiary amino functional groups in the repeating unit that impart certain chemical properties to the polymer like, e.g., those of a weak base. These chemical properties may lead to degradation of the mechanical properties, in addition to increase in weight, on chemical reaction (e.g., with CO_2 and atmospheric pollutants). The association and subsequent reaction of the amino groups with molecules of water may have an effect on the NMR line observed with the soaked polymer that was recently ascribed to a state of the water molecules "perhaps hydrogen bonded to the polymer" (ref. 14). In addition to the amino functional group there are two additional functional groups in the repeating unit: the -OH (hydroxyl) and the $-SO_2$ (sulfonyl) functional groups. The presence of functional groups may also be important in the determination of transients formed after the transfer of energy from ionizing radiation to a polymer. Since electrons penetrate into matter deepest and are the primary constituents of the space ionizing radiation, and since all ionizing radiation in space leads to the formation of secondary electrons on interaction with matter, it is of general interest to investigate the effect of electron impact on molecules first. From this viewpoint it is of interest to study the role of functional groups in electron impact fragmentation of molecules. Because of the predominant production of positive ions (usually, but not always, by orders of magnitude) over that of negative ions on electron-impact and the larger availability of mass spectra for positive ions, this investigation started with positive ions first. However, the possibility of an important role for negative ions should not be discounted.

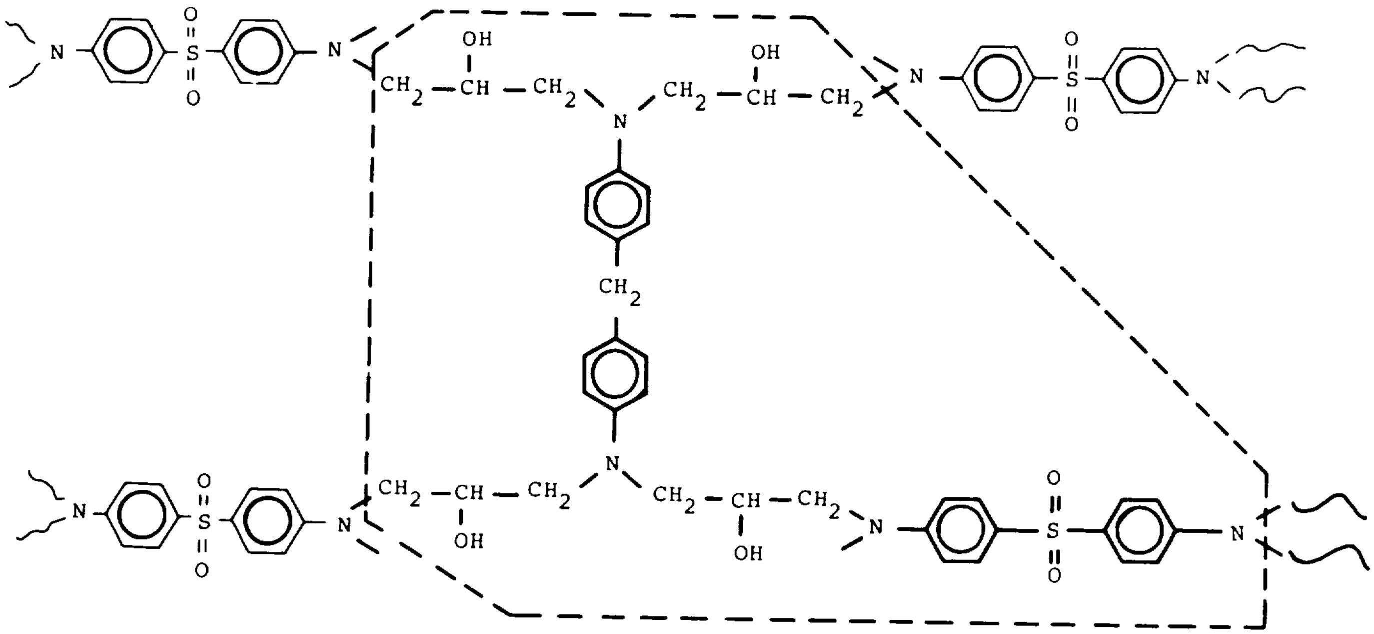

ELECTRON-IMPACT MASS SPECTRA OF MOLECULES WITH AN AMINO GROUP

Mass spectra of some molecules that contain amino functional groups are shown (ref. 15). It has been observed experimentally that among several chemical functional groups, including the hydroxyl and amino groups, that are present as substituents in aliphatic chemical compounds the amino functional group influences the chemical bond scission and ionization on electron impact the most strongly (refs. 16-17). The extent of substitution on the amino group itself appears to increase the influence of the amino group on the dissociative ionization. The dominant bond scission is that between α and β carbon atoms in hydrocarbon chains, leading to the formation of imonium ions. In aromatic amines with no α and β carbon atoms in aliphatic groups the parent ion or the alkyl substituted amino group ion may be formed predominantly.

93 C_6H_7N 62-53-3
Benzenamine

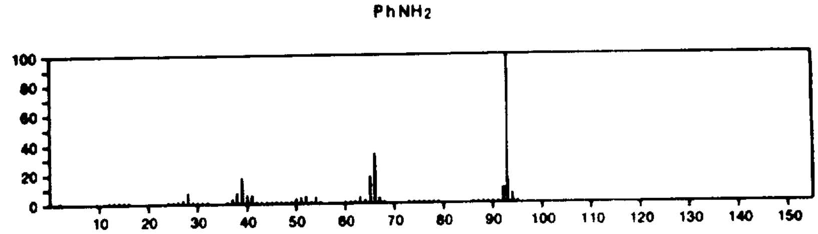

149 $C_{10}H_{15}N$ 91-66-7
Benzenamine, *N,N*-diethyl-

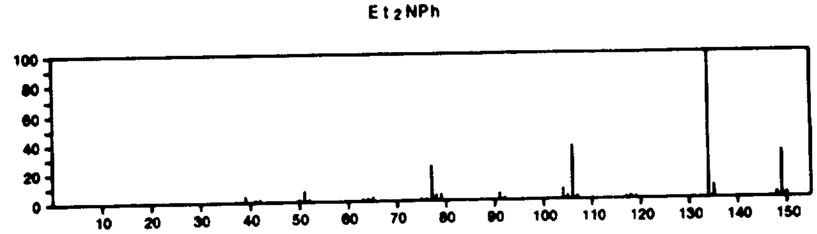

177 $C_{12}H_{19}N$ 53927-61-0
Benzenamine, *N*-(2,2-dimethylpropyl)-*N*-methyl-

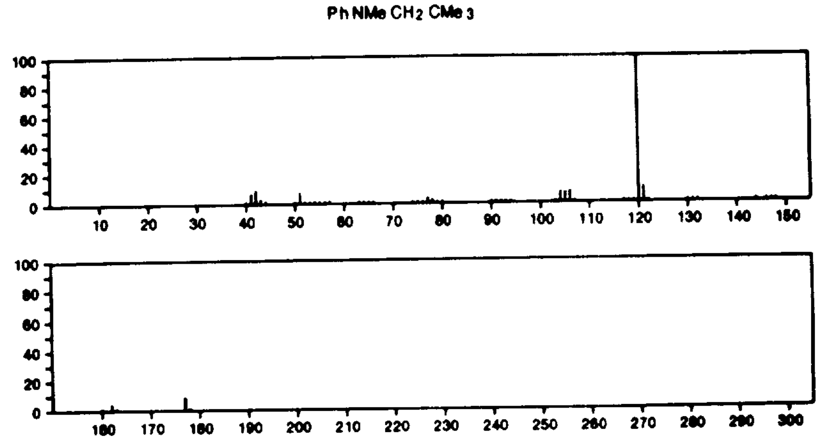

ELECTRON-IMPACT MASS SPECTRA OF LARGE MOLECULES WITH AMINO GROUPS

Structural formulae and electron-impact mass spectra are shown for additional molecules that have amino functional groups as their substituents and, in addition, appear to be constituents to some extent of the repeating unit in the structure of the polymer. The fragmentation pattern on electron-impact of these and other compounds to be investigated may lead to the identification of some of the sites of bond scission and of ions and radicals that may be formed under the action of ionizing radiation on the polymer.

198 $C_{13}H_{14}N_2$ **101-77-9**

Benzenamine, 4,4'-methylenebis-

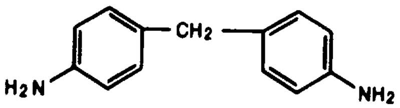

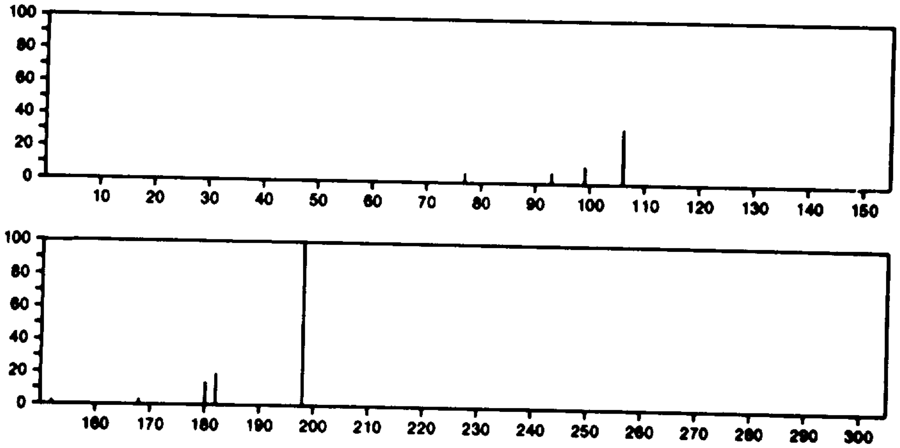

268 $C_{17}H_{20}N_2O$ **90-94-8**

Methanone, bis[4-(dimethylamino)phenyl]-

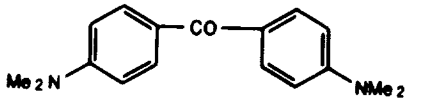

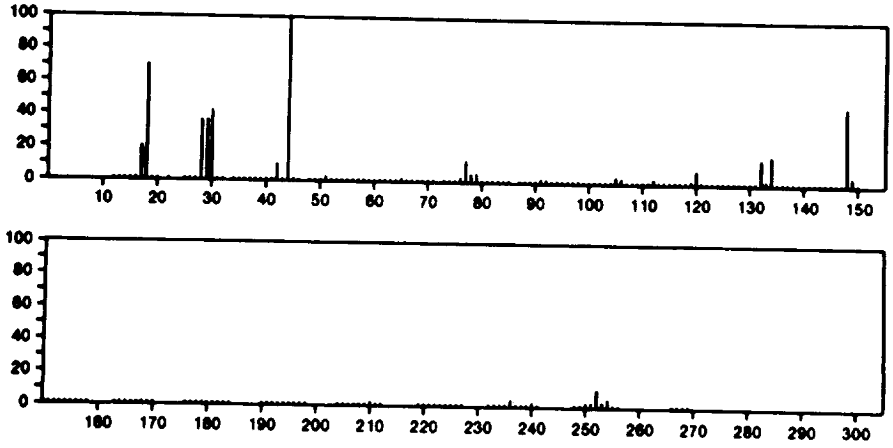

ELECTRON-IMPACT MASS SPECTRA OF MOLECULES WITH A HYDROXYL GROUP

The electron-impact mass spectra of several molecules that contain the hydroxyl functional group are shown. The hydroxyl group in aliphatic compounds appears to favor ionization and scission of the bond between α and β carbon atoms with respect to the hydroxyl group, although much less dominantly compared to the amino group.

198 $C_{14}H_{14}O$ **614-29-9**

Benzeneethanol, α-phenyl-

$PhCH_2CH(OH)Ph$

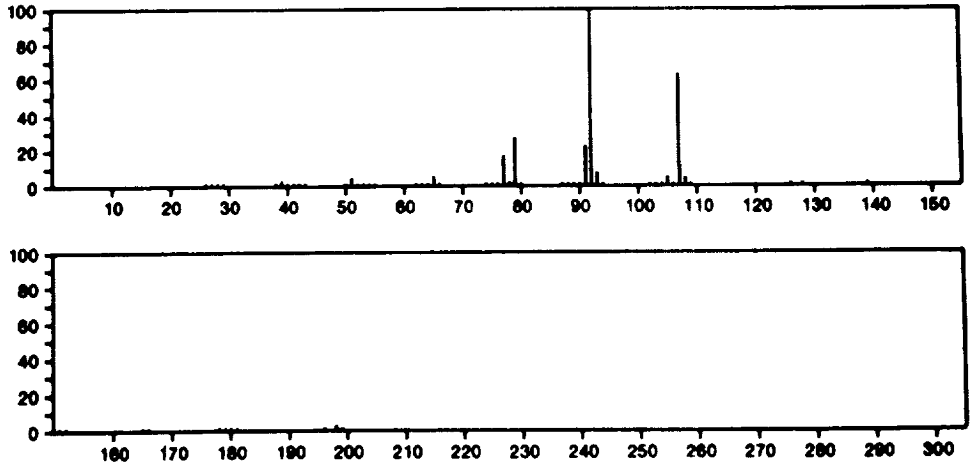

192 $C_{13}H_{20}O$ **7661-43-0**

Phenethyl alcohol, α-butyl-β-methyl-

$Me(CH_2)_3CH(OH)CHMePh$

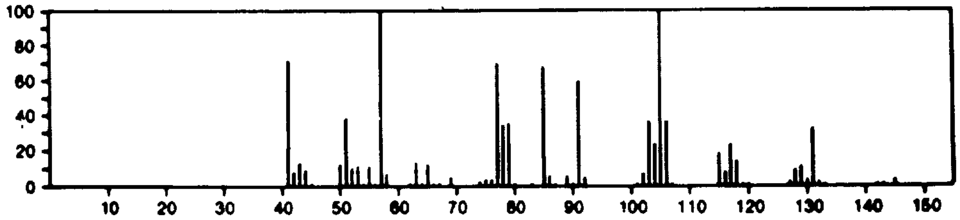

ELECTRON-IMPACT MASS SPECTRA OF MOLECULES WITH BOTH A HYDROXL AND AN AMINO GROUP

When both an amino group and a hydroxyl group are present in a molecule, the amino group appears to form a more abundant, if not the most abundant, fragment ion on electron-impact, namely the $=C=NH^+$ (imonium ion) compared to the $=C=OH^+$ (oxonium ion), the ion from the hydroxyl group.

75 C_3H_9NO 78-91-1

1-Propanol, 2-amino-

$HOCH_2CH(NH_2)Me$

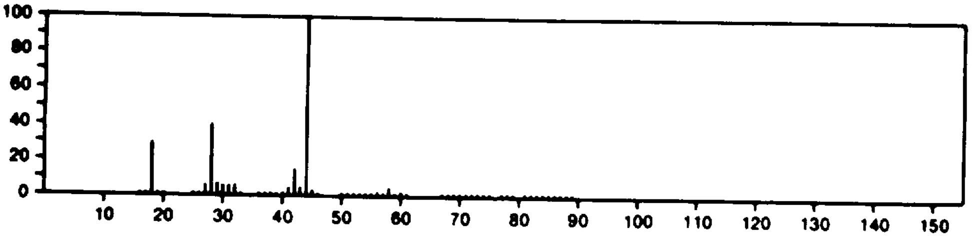

75 C_3H_9NO 78-96-6

2-Propanol, 1-amino-

$H_2NCH_2CH(OH)Me$

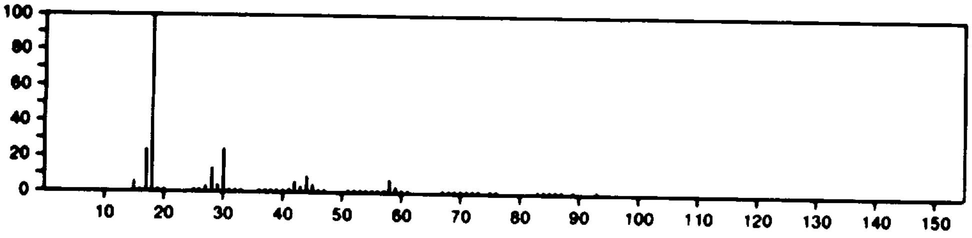

75 C_3H_9NO 156-87-6

1-Propanol, 3-amino-

$H_2N(CH_2)_3OH$

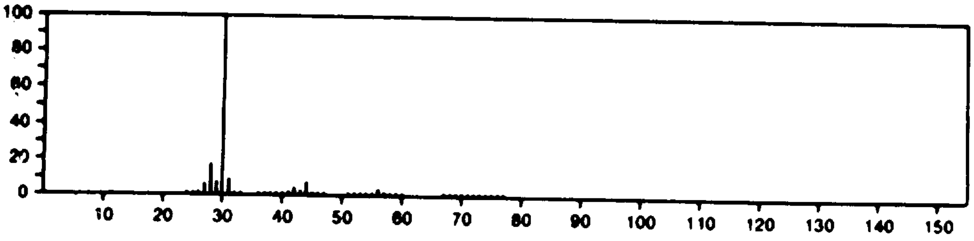

ELECTRON-IMPACT MASS SPECTRA OF MOLECULES WITH A SULFONYL GROUP

The electron-impact mass spectra of certain molecules that contain the $-SO_2-$ functional group are also shown. Ions formed by scission of C-S and S-O bonds appear to form in addition to the parent ion. The nature of the substituents influences the dissociative ionization involved.

248 $C_{12}H_{12}N_2O_2S$ **80-08-0**

Benzenamine, 4,4'-sulfonylbis-

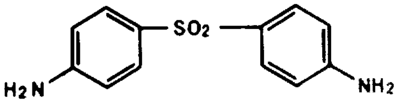

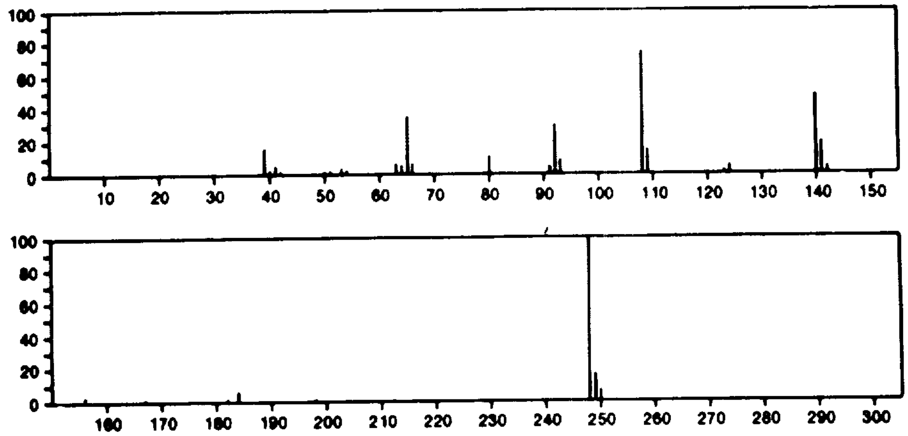

---

218 $C_{12}H_{10}O_2S$ **127-63-9**

Benzene, 1,1'-sulfonylbis-

PhSO2Ph

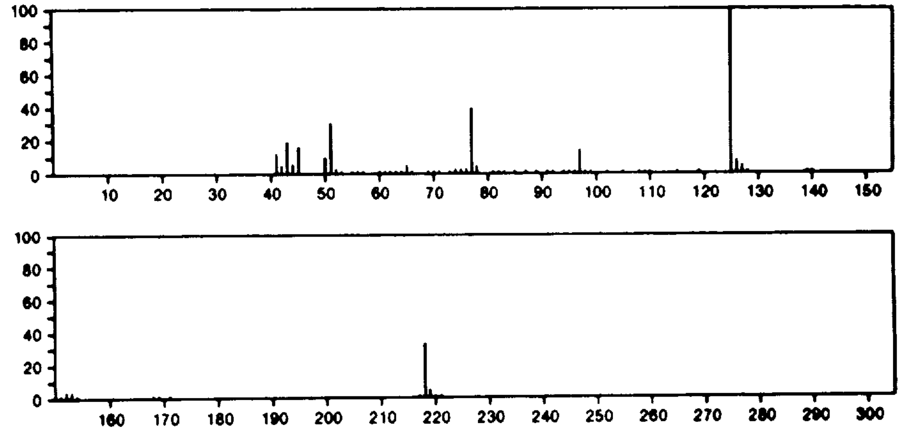

SITES OF MAJOR DISSOCIATIVE IONIZATION ON THE POLYMER ACCORDING TO ELECTRON-IMPACT MASS SPECTRA

Sites of possible major ionization and bond scission are shown on a repeating unit of the polymer formed by curing tetraglycidyl methylenedianiline with diamino diphenyl sulfone. The determination of possible sites is based on electron-impact mass spectrometric evidence.

SITES OF MAJOR DISSOCIATIVE IONIZATION ACCORDING TO ELECTON-IMPACT MASS SPECTRA

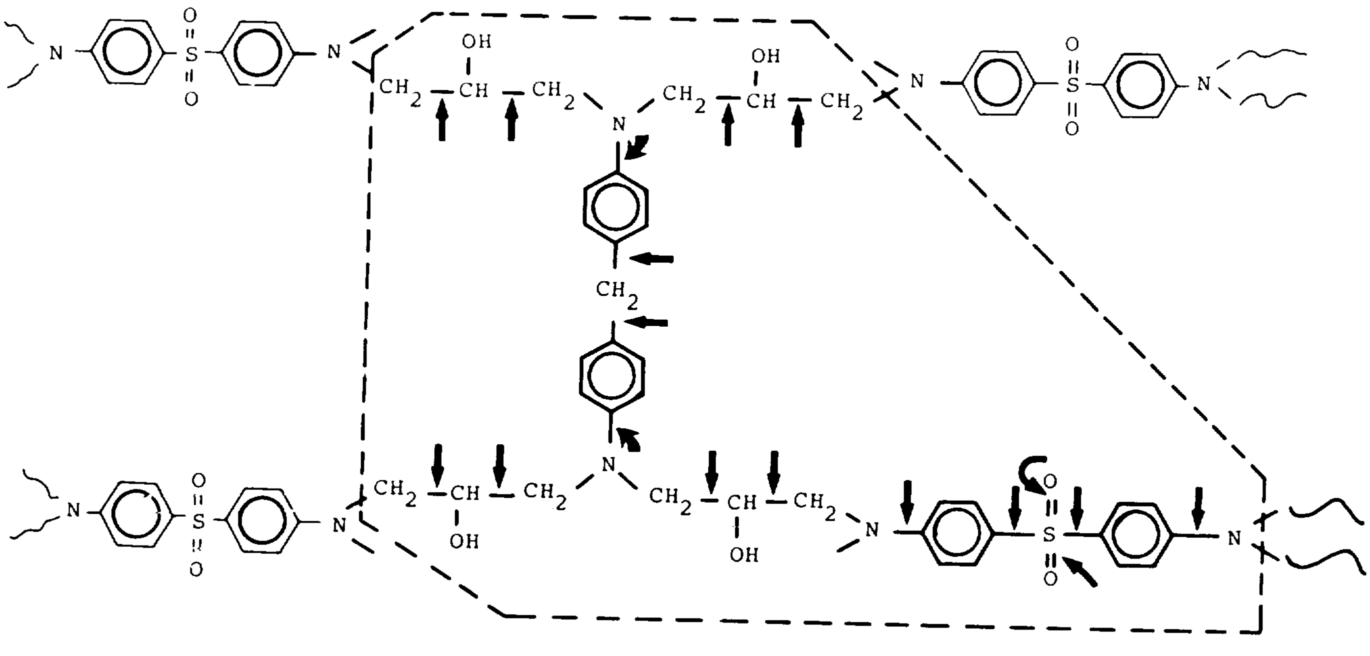

LONGITUDINAL ENERGY ABSORPTION FOR PROTONS PENETRATING INTO THE POLYMER AND A COMPOSITE MATERIAL OF THE POLYMER

The density of chemically active species is of utmost importance in determining the chemical products within an activated region since they affect the rates of various competing chemical reactions. We shall now consider the spatial inhomogeneity of the initial energy deposit. The energy absorption as a function of penetration depth is shown for monoenergetic protons of three energy levels. It has been calculated according to the stopping power of Anderson and Ziegler (ref. 18). The energy deposit per unit volume is quite high due to the proton's low speed and limits the penetration to short distances (note that the penetration depth is expressed in units of areal density which is the distance of penetration times the material density). Penetration depths and energy deposit in this graph for low energy protons should be compared with electron data of the following graph.

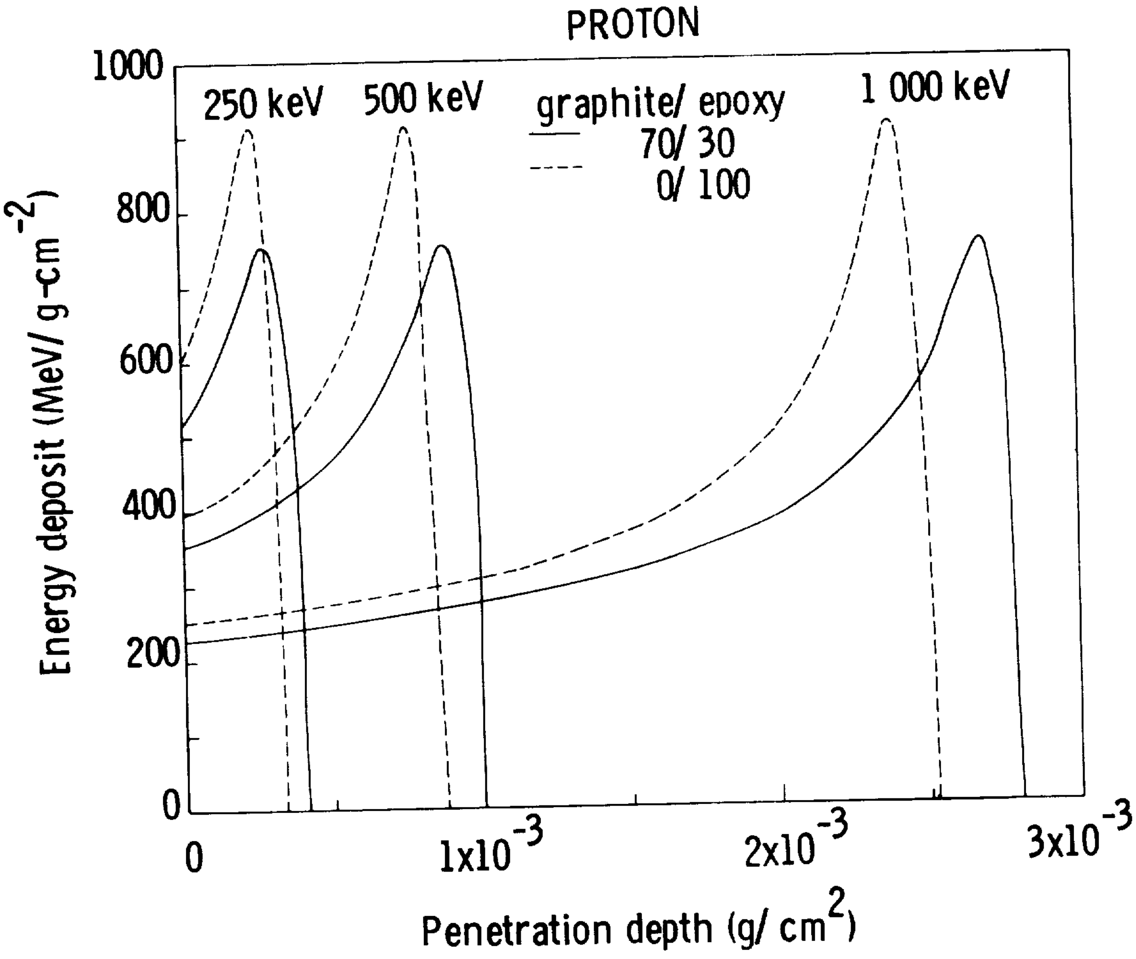

LONGITUDINAL ENERGY ABSORPTION FOR PASSAGE OF ELECTRONS THROUGH THE POLYMER AND A COMPOSITE MATERIAL OF THE POLYMER

The energy absorption for electrons is more dispersed in the material as a result of the electron's smaller mass and higher velocity. Shown here is the distribution of energy deposit as a function of penetration depth calculated according to the electron transmission coefficient and average transmitted energy (ref. 19). The declining peak values as a function of depth results from the increased multiple scattering of the electrons randomizing their direction of travel at larger depths. Such effects are of principal importance in defining dose profiles within the material.

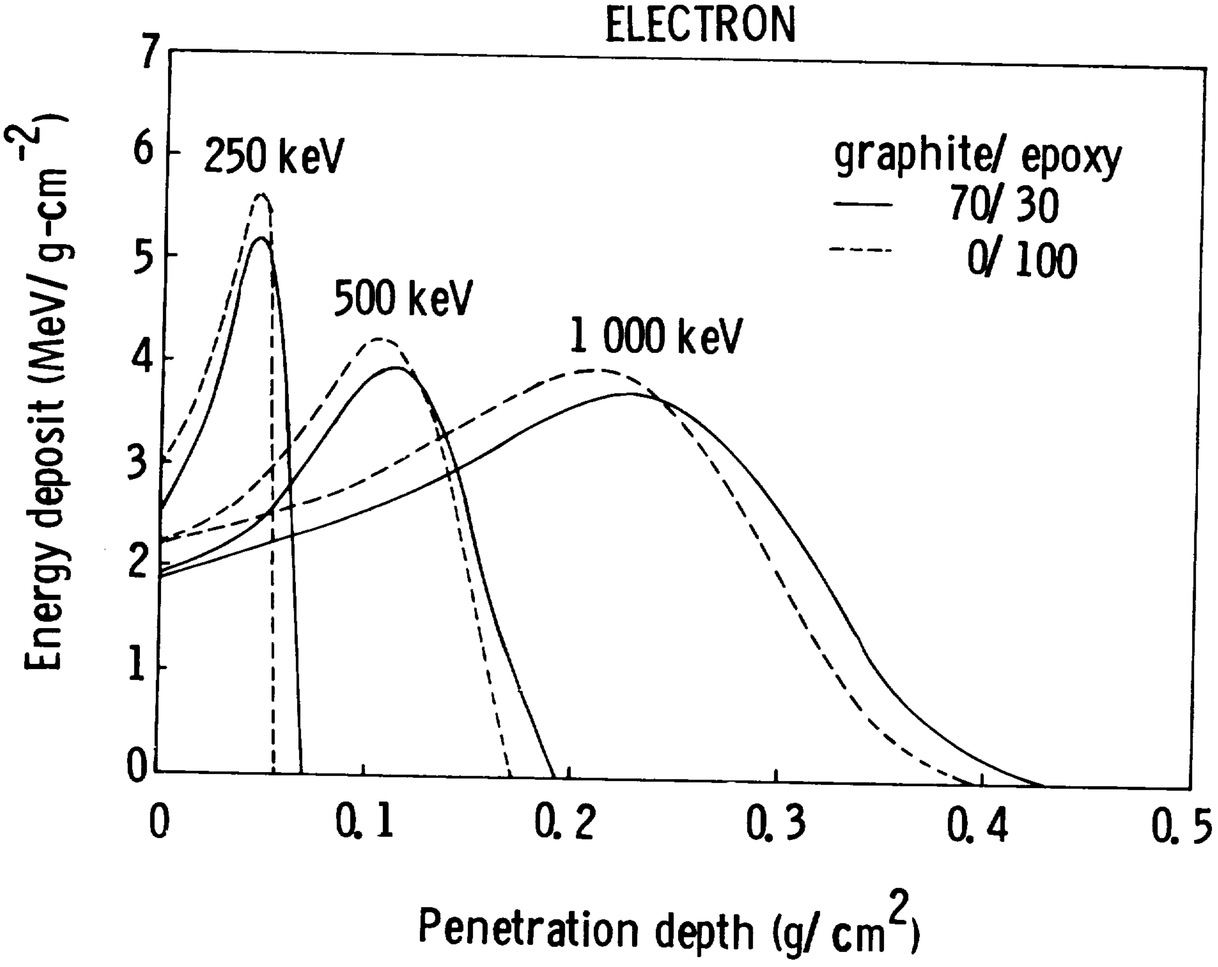

EXCITATION AND IONIZATION DENSITY NEAR A 100-KeV-PARTICLE PATH

The lateral dispersion of the energy deposit extends over two energy absorption regions, the core and the penumbra. In the core, the energy transferred from a passing charged particle to a material shows radial dependence that depends on the mechanism of the coulombic interaction considered. One process involves the coulombic interaction between the charged particle and the electron of one individual atom or molecule, in which case the radial dependence of the energy transferred is given approximately (ref. 5a) by equation (1). Another process involves the collective longitudinal excitation of valence electrons of the atoms or molecules in the condensed phase, in which case the radial dependence is given approximately (ref. 5b) by equation (2) (for singly charged projectiles)

$$P_n \approx \exp(-E_n r/3hv) \qquad (1)$$

$$\rho(r) \approx \exp(-2\omega_p r/v)/r^2 \qquad (2)$$

Clearly, the highest energy transfers are restricted to small radial distances. Even so the highest energy transfers result in energetic secondary electrons which generally travel far from their sites of production and deposit their energy far from the trajectory of the original passing particle forming a penumbra of energy deposited outside the core region. The core and penumbra of 100 KeV protons and electrons are shown clearly in the graph. The core region of the proton is limited to a few atomic distances by the proton's low velocity while the electron core to about 6 nm according to equation (1). The proton-produced penumbra is limited by the secondary electron mass to proton mass ratio, which limits the energy transferred to secondary electrons. The electron produced penumbra extends far off the graph to the right. There are great differences between the excitation densities achieved by the passage of the two particles. Without doubt, rapid recombination will characterize the chemistry in the proton's core region. A more detailed analysis is required to better define the chemistry of these various regions of exposure.

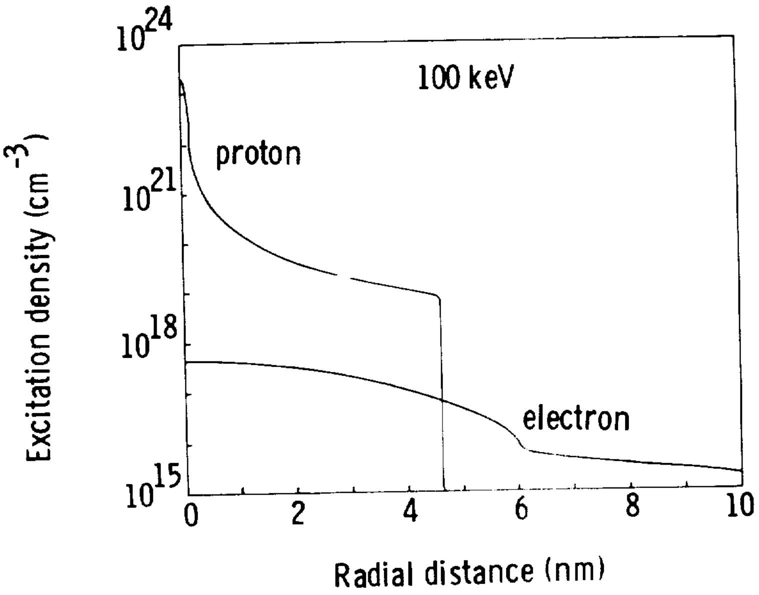

EXCITATION AND IONIZATION DENSITY NEAR A 1000-KeV-PARTICLE PATH

At higher particle energy the same features are apparent in the track structure but the radial distances are expanded. The proton core region still appears on the graph but the electron core extends to the right of the present graph. Qualitatively, we anticipate the proton core chemistry to be radically different from the remainder of the exposed regions. The chemical change in any solid material will be limited to a small cylindrical region around the individual particle trajectory. Early in the exposure these cylindrical regions will not overlap and their evolution will develop independently of one another. Late in the exposure of highly irradiated material the chemistry of later tracks will generally be altered by the prior change of the material caused by a previous track.

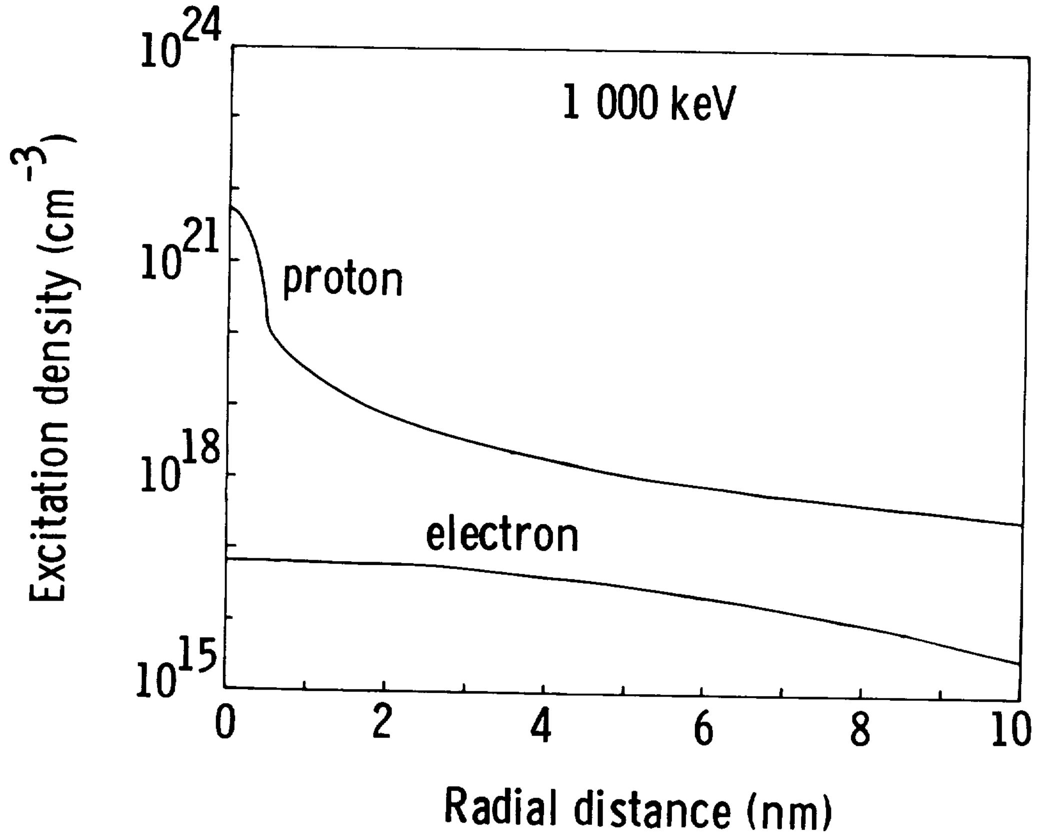

GEOSTATIONARY DOSE IN ORGANIC COMPOSITES SHOWING GEOMETRIC AND MODEL UNCERTAINTIES

The accumulated 30 year dose for geostationary orbit is shown in the graph. It is represented by exposure of ≈ 10^{11} rad at ≈ 0.5 μ depths due to low energy protons and ≈ 5×10^9 rad at ≈ 50 μ due to electrons. At these values, each portion of material receives energy by the near passage of several particles. Two effects could result from such multiple track exposure: (a) if sufficiently close in time, then chemically active species of the two trajectories may alter the chemical end product; (b) even if long times elapsed between the passage of the two particles then the second passes through previously altered material. Of interest is the number of traversals which overlap within a given time interval for an accelerated test of the 30-year geostationary exposure.

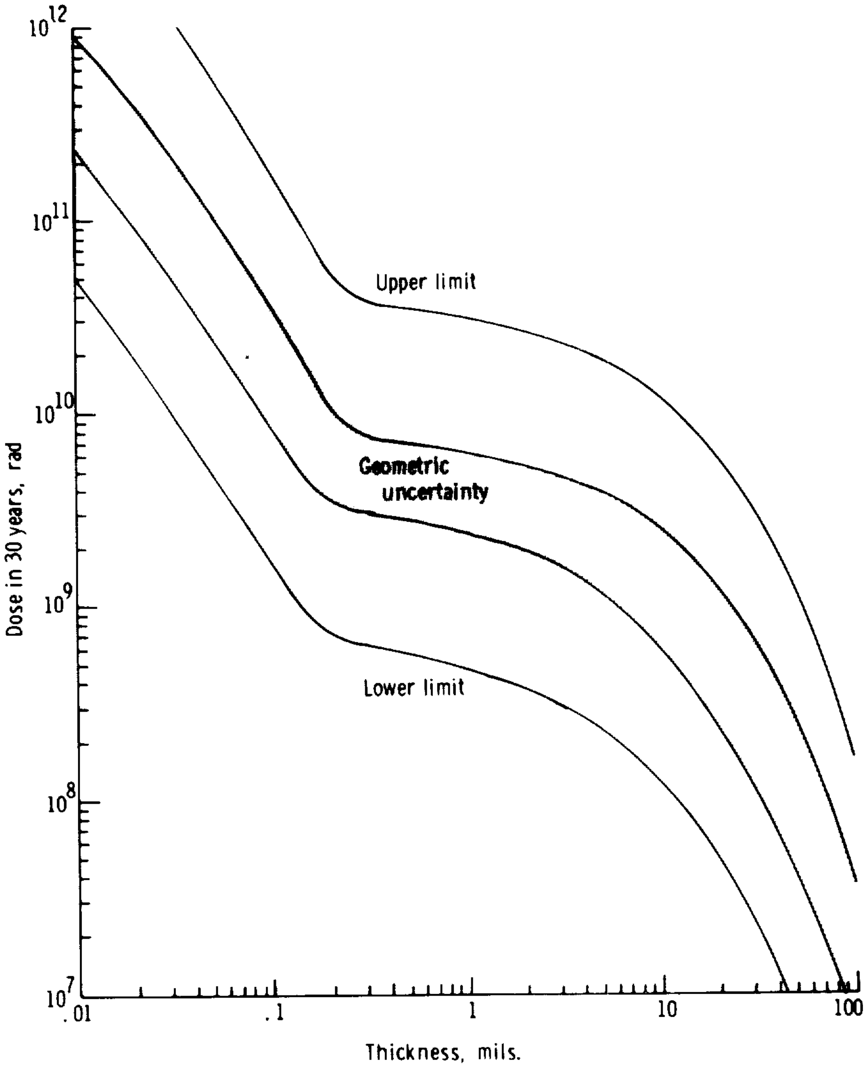

PROBABILITY OF OVERLAP OF TWO-PARTICLE TRACKS WITHIN TIME Δt (30-YEAR GEOSTATIONARY EXPOSURE ACCELERATED BY 10^4)

The probability of overlap of two particle tracks within a time interval Δt is shown for an accelerated test at 30 year geostationary exposure levels. The test is assumed completed in one day (24 hours). It is seen that the more active chemical species ($\Delta t \approx 1$ μsec) will rarely be affected by such events. A small effect is expected for the slow chemical processes ($\Delta t \approx 1$ msec) in the penumbra region of the electron exposure. Effects on long lived radicals ($\Delta t = 1$ sec) are likely in nearly all regions. Most of the exposure is seen to take place in previously disturbed material ($\Delta t \approx$ 1 day). What is clear from these figures is that material changes result from the combined effects of spatially compact individual particle tracks.

	PROTON		ELECTRON	
ΔT	CORE	PENUMBRA	CORE	PENUMBRA
1 μSEC	3×10^{-11}	3×10^{-8}	5×10^{-7}	2×10^{-5}
1 MSEC	3×10^{-8}	3×10^{-5}	5×10^{-4}	2×10^{-2}
1 SEC	3×10^{-5}	3×10^{-2}	5×10^{-1}	≈ 1
1 DAY	≈ 1	≈ 1	≈ 1	≈ 1

SUMMARY AND CONCLUSIONS

- A useful model of charged particle impact with the polymer has been presented.
- Principal paths of molecular relaxation have been identified.
- The radiation-induced changes will be confined to local regions about individual particle tracks.
- The main additional effects of accelerated testing may result from effects because of possible higher temperatures and long-lived free radicals.
- Chemically active source terms are now reasonably defined. Attention must now be given to subsequent processes.

References

1. a. Rosenstock, H. M.; Wallenstein, M. B.; Wahrhaftig, A. L.; and Eyring, H.: Absolute Rate Theory for Isolated Systems and the Mass Spectra of Polyatomic Molecules. Proc. Natl. Acad. Sci. U.S., vol. 38, 1952, pp. 667-678. b. Rosenstock, H. M.: Theory of Mass Spectra. A General Review. Adv. Mass Spectrom, vol. 4, 1968, pp. 523-545.

2. Kupperman, A.: Diffusion Model of the Radiation Chemistry of Aqueous Solutions. Radiation Research, North-Holland Pub., 1967, pp. 212-234.

3. Bethe, Hans A.: Zur Theorie der Durchgangs schneller Korpurskularstrahlen durch Materie. Ann. Physik, vol. 5, 1930, pp. 325-400.

4. Platzman, Robert J.: Influences of Details of Electronic Binding on Penetration Phenomena, and the Penetration of Energetic Charged Particles through Liquid Water. Symposium on Radiobiology; The Basic Aspects of Radiation Effects on Living Systems (Oberlin College, June 14-18, 1950), 1952, pp. 139-173.

5. a. Wilson, John W.: Solar-Pumped Gas Laser Development. NASA TM 81894, December 1980. b. Ritchie, R. H.; and Brandt, Werner: Primary Processes and Track Effects in Irradiated Media. Radiation Research; Biomedical, Chemical and Physical Perspectives. Academic Press, Inc., 1975, pp. 315-324.

6. Katz, R.; Ackerson, B.; Homayoonfar, M.; and Sharma, S. C.: Inactivation of Cells by Heavy Ion Bombardment. Radiation Res., vol. 47, 1971, pp. 402-424.

7. Lindhard, J.; and Scharff, M.: Recent Developments in the Theory of Stopping Power. Principles of the Statistical Method. Penetration of Charged Particles in Matter (Conference at Gatlinburg, Tennessee, September 15-18, 1958.). NAS-NRC Publ. 752, 1960, pp. 49-55.

8. Gordon, R. G.; and Kim, Y. S.: Theory for the Forces Between Closed-Shell Atoms and Molecules. J. Chem. Phys., vol. 56, 1972, pp. 3122-3133.

9. Wilson, John W.; and Kamaratos, Efstathios: Mean Excitation Energy for Molecules of Hydrogen and Carbon. Phys. Lett., vol. 85A, 1981, pp. 27-29.

10. Wilson, J. W.; Chang, C. K.; Xu, Y. J.; and Kamaratos, E.: Ionic Bond Effects on Mean Excitation Energy for Stopping Power. To be published in J. Appl. Phys., Feb. 1982.

11. Bragg, W. H.; and Kleeman, R.: On the α Particle of Radium and their Loss of Range in passing through various atoms and molecules. Philos. Mag., vol. 10, 1095, pp. 318-340.

12. Dehmer, J. L.; Inokuti, M.; and Saxon, R. P.: Systematics of moments of dipole oscillator-strength distributions for atoms of the first and second row. Phys. Rev., vol. 12A, 1975, pp. 102-121.

13. Long, E. R., Jr.: Electron and Proton Absorption Calculations for a Graphite/Epoxy Composite Model. NASA Technical Paper 1568. November 1979, p. 16.

14. Lawing, D.; Fornes, R. E.; Gilbert, R. D.; and Memory, J. D.: Temperature dependence of broadline NMR spectra of water-soaked, epoxy graphite composites. J. Appl. Phys., vol. 52, 1981, pp. 5906-5907; and references therein.

15. Heller, S. R.; and Milne, G. W. A. (eds.): EPA/NIH Mass Spectral Data Base; 1980 Cumulative Indexes. NSRDS-NBS 63, Suppl. 1.

16. Remberg, G.; Remberg, E.; Spiteller-Friedmann, M.; and Spiteller, G.: Massenspektren Schwach Angeregter Moleküle. 4. Mitteilung. Org. Mass Spectrom., vol. 1, 1968, pp. 87-113.

17. Remberg, G.; and Spiteller, G.: Über den Einfluss von Substituenten auf die primären Abbaureaktionen aliphatischer Verbindungen im Massenspectrometer. Chem. Ber., vol. 103, 1970, pp. 3640-3660.

18. Anderson, H. H.; and Ziegler, J. F.: The Stopping and Ranges of Ions in Matter. Vol. 3. Hydrogen Stopping Powers and Ranges in All Elements. Pergamon Press, 1977.

19. Mar, B. W.: An Electron Shielding Analysis for Space Vehicles. Nucl. Sci. and Eng., vol. 24, 1966, pp. 193-199.